

Cite this: *Phys. Chem. Chem. Phys.*, 2012, **14**, 11027–11039

www.rsc.org/pccp

PAPER

Recognition-driven layer-by-layer construction of multiprotein assemblies on surfaces: a biomolecular toolkit for building up chemoresponsive bioelectrochemical interfaces†

Diego Pallarola,^a Catalina von Bilderling,^b Lía I. Pietrasanta,^{bc} Nuria Queralto,^d Wolfgang Knoll,^e Fernando Battaglini^{*cf} and Omar Azzaroni^{*ac}

Received 17th April 2012, Accepted 29th May 2012

DOI: 10.1039/c2cp41225j

The development of soft bioelectronic interfaces with accurate compositional and topological control of the supramolecular architecture attracts intense interest in the fast-growing field of bioelectronics and biosensing. The present study explores the recognition-driven layer-by-layer assembly of glycoenzymes onto electrode surfaces. The design of the multi-protein interfacial architecture is based on the multivalent supramolecular carbohydrate–lectin interactions between redox glycoproteins and concanavalin A (Con A) derivatives. Specifically, [Os(bpy)₂Clpy]²⁺-tagged Con A (Os-Con A) and native Con A were used to direct the assembly of horseradish peroxidase (HRP) and glucose oxidase (GOx) in a stepwise topologically controlled procedure. In our designed configuration, GOx acts as the biorecognition element to glucose stimulus, while HRP acts as the transducing element. Surface plasmon resonance (SPR) spectroscopy and quartz crystal microbalance with dissipation (QCM-D) results are combined to give a close representation of the protein surface coverage and the content of water in the protein assembly. The characterization is complemented with *in situ* atomic force microscopy (AFM) to give a topographical description of the layers assemblage. Electrochemical (EC) techniques were used to characterize the functional features of the spontaneously self-assembled biohybrid architecture, showing that the whole system presents efficient electron transfer and mass transport processes being able to transform micromolar glucose concentration into electrical information. In this way the combination of the electroactive and nonelectroactive Con A provides an efficient strategy to control the position and composition of the protein layers *via* recognition-driven processes, which defines its sensitivity toward glucose. Furthermore, the incorporation of dextran as a permeable interlayer able to bind Con A promotes the physical separation of the biochemical and transducing processes, thus enhancing the magnitude of the bioelectrochemical signal. We consider that these results are relevant for the nanoconstruction of functional biointerfaces provided that our experimental evidence reveals the possibility of locally addressing recognition, transduction and amplification elements in interfacial ensembles *via* LbL recognition-driven processes.

^a Instituto de Investigaciones Físicoquímicas Teóricas y Aplicadas (INIFTA), Departamento de Química, Facultad de Ciencias Exactas, Universidad Nacional de La Plata, CONICET, CC 16 Suc. 4, 1900 La Plata, Argentina. E-mail: azzaroni@inifta.unlp.edu.ar; Web: <http://softmatter.quimica.unlp.edu.ar>

^b Centro de Microscopías Avanzadas (CMA), Facultad de Ciencias Exactas y Naturales, Universidad de Buenos Aires, Ciudad Universitaria, Pabellón 1, C1428EHA, Buenos Aires, Argentina

^c Consejo Nacional de Investigaciones Científicas y Técnicas, C1033AAJ, Buenos Aires, Argentina

^d Max-Planck-Institut für Polymerforschung, Ackermannweg 10, 55128 Mainz, Germany

^e Austrian Institute of Technology (AIT), Donau-City-Strasse 1, 1220 Vienna, Austria

^f INQUIMAE, Departamento de Química Inorgánica, Analítica y Química Física, Facultad de Ciencias Exactas y Naturales, Universidad de Buenos Aires, Ciudad Universitaria, Pabellón 2, C1428EHA, Buenos Aires, Argentina. E-mail: battaglini@qi.fcen.uba.ar

Web: <http://www.qi.fcen.uba.ar/personales/battaglini.htm>

† Electronic supplementary information (ESI) available. See DOI: 10.1039/c2cp41225j

Introduction

Interfacial supramolecular assemblies generated in a layer-by-layer (LbL) fashion have found an incredible resonance and a vast number of applications in many scientific areas during the past decades.^{1,2} An essential cornerstone for the construction of multicomponent interfacial architectures is the development of methods for integrating molecular building blocks into well-defined organized assemblies. In most of the cases, such interfacial architectures require accurate control of composition as well as of molecular orientation and organization at the nanometer scale. One major attraction of LbL assembly is its potential for the combination of diverse building blocks of complementary affinities to create thin films on solid substrates displaying functional groups at controlled sites in nanoscale arrangements. During the early days, LbL assembly was almost exclusively based on multilayered polyelectrolyte assemblies, in which electrostatic attraction was the main driving force leading to the film growth.³ Thereafter, the hoped-for influx of new approaches certainly happened and the LbL method was successfully extended to other driving forces such as hydrogen bonding, charge transfer, host–guest interactions, acid–base pairs, metal–ion coordination, and biospecific interactions.⁴ In this regard, those biospecific ligand–receptor interactions have proven to be very efficient in assembling different biological functional units on surfaces.⁵ The use of multivalent bio-supramolecular interactions to promote directional and selective self-assemblies of proteins represents a research topic of growing relevance in supramolecular surface chemistry.^{6,7}

In a similar vein, multilayer assemblies containing redox-active proteins are also attracting widespread interest within the scientific community as versatile architectures to create chemo-responsive biointerfaces or even biomimetic signal transfer systems. Recent work of Lisdat and co-workers illustrates the potential of self-assembling all-protein interfacial architectures incorporating intrinsically electroactive biomolecules in order to create biomimetic signal chains.⁸ These authors demonstrated the creation of electrostatic bioassemblies displaying remarkable functional features constituted of cytochrome *c*, as a redox mediator, and sulfite oxidase or bilirubin oxidase, as sensing elements. For instance, the integration of redox glycoproteins on conductive supports has enabled the design of bioelectrochemical interfaces capable of molecular recognition. The electrical signal triggered by the enzyme can be integrated into circuits leading to biosensors, miniaturized labs-on-chips, bimolecular microelectronics, or biofuel cells.⁹ Recently, we have demonstrated that redox-tagged Con A, a protein displaying carbohydrate-binding sites,¹⁰ can be used not only as “biosupramolecular glue” facilitating the robust and easy attachment of HRP onto electrodes without affecting its catalytic activity but also as an electron-conducting phase enabling the electrical communication between the prosthetic group of the enzyme and the electrode support.¹¹

Here we propose an alternative strategy for attaining multi-protein interfacial architectures, thus leading to the formation of highly versatile enzymatic electrodes. The stepwise construction of the bioactive self-assembled multilayers was accomplished on the basis of multivalent supramolecular carbohydrate–lectin interactions between glycoproteins (HRP and GOx) and

Con A derivatives.^{12,13} The use of redox-active Con A as a biorecognizable platform enabling the spontaneous assembly and electrical wiring of multiple glycoenzyme layers onto electrodes remains an unexplored research topic in contemporary supramolecular science and, consequently, we devoted particular attention to explore these features. The experimental results reveal that the combination of electroactive and nonelectroactive lectins facilitates the nanoscale control over the positioning of the glycoenzyme layers, which in turn promotes a better coupling between biochemical and electron transfer processes taking place within the supramolecular assembly. The positioning and composition of the protein layers can be easily controlled *via* recognition-driven processes between the biofunctional units displaying ligand or receptor characteristics and have a strong influence on the magnitude of the bioelectrochemical signal obtained in the presence of the chemical stimulus.

Experimental

Materials

Canavalia ensiformis Concanavalin A (Con A, jack bean), cystamine dihydrochloride (Cys), α -D-mannopyranosylphenyl isothiocyanate (Man), β -D-glucose, 40 kDa dextran from *Leuconostoc* spp. and horseradish peroxidase (HRP) (type VI; RZ = 3.1) were purchased from Sigma. $[(\text{Os}(\text{bpy})_2\text{Clpy})^+ - \text{PEG}]_{12}$ -Con A (Os-Con A) was synthesized as previously described,¹⁴ where bpy stands for bipyridine, py for pyridine and PEG for a 336 Da MW polyethylene glycol. Glucose oxidase (GOx, *Aspergillus niger*) was obtained from Calzyme Laboratories, Inc. All other reagents were of analytical grade.

Construction of self-assembled layers

The construction of molecular assemblies was achieved by using a BK7 glass coated with 2 nm of chromium and 50 nm of gold by evaporation. The substrate was incubated overnight with a solution of cystamine dihydrochloride (5 mM) in ethanol, then the electrode was rinsed with ethanol and dried with N_2 , followed by 2 h incubation in a solution of α -D-mannopyranosylphenyl isothiocyanate ($10 \mu\text{g mL}^{-1}$) in PBS buffer (0.05 M, pH 7.4). Then the electrode was rinsed with PBS buffer and immersed for 1 h in a solution of Con A or Os-Con A (1 μM) in PBS buffer containing CaCl_2 (0.5 mM) and MnCl_2 (0.5 mM). The same buffer was used to incorporate the HRP, GOx and dextran onto the surface and to rinse the electrode after a Con A, Os-Con A, dextran, HRP or GOx assembling step. To immobilize the enzymes onto the lectin-modified surface, the electrode was incubated in the corresponding enzyme solution (1 μM) for 1 h. The incorporation of the dextran was achieved under the same conditions described for the enzymes. All steps were carried out at RT (*ca.* 22 °C).

Quartz crystal microbalance with dissipation monitoring

The QCM-D measurements were carried out at 21 °C using a Q-Sense E1 microbalance (Q-Sense, Göteborg, Sweden). This instrument allows for a simultaneous measurement of frequency change (Δf) and energy dissipation change (ΔD) by periodically switching off the driving power of the oscillation of the sensor crystal and by recording the decay of the damped oscillation.

The time constant of the decay is inversely proportional to D , and the period of the decaying signal gives f . Experiments were performed using commercially available (QSX-301, Q-Sense) gold-coated quartz crystals.

Surface plasmon resonance spectroscopy

SPR detection was carried out in a homemade device using the Kretschmann configuration.¹⁵ The SPR substrates were BK7 glass slides evaporation-coated with 2 nm of chromium and 50 nm of gold. Prior to and after injection of protein solution into the liquid cell a measurement of the SPR signal at different angles was recorded. This has been done in order to detect the shift of the minimum angle of reflectance due to the protein bioconjugation on the surface. The SPR angle shifts were converted into mass uptakes using the experimentally determined relationship, $\Gamma(\text{ng mm}^{-2}) = \Delta\theta(^{\circ})/0.19$. The sensitivity factor was obtained following procedures reported in the literature.¹⁶

Electrochemical measurements

Cyclic voltammetry and chronoamperometry experiments were performed with a μ Autolab potentiostat (Echo Chemie) using a three-electrode cell equipped with an Ag/AgCl reference electrode and a platinum mesh counter electrode. All electrochemical experiments were carried out at room temperature (*ca.* 22 °C) in a Teflon cell designed to expose 0.18 cm² of the surface of the electrode to the solution. Electrochemical experiments were carried out in a 0.05 M KH₂PO₄/K₂HPO₄, 0.1 M KNO₃ buffer solution at pH 7.4 under an oxygen atmosphere.

Atomic force microscopy imaging

Tapping-mode AFM in liquid was performed using a NanoScope IIIa-Quadrex Multimode-AFM (Bruker, CA) with a vertical J scanner having a maximal lateral range of approximately 150 μm . After a period of 15 to 30 min of thermal relaxation, initial engagement of the tip was achieved at scan size zero to minimize sample deformation and tip contamination. SNL AFM probes (Bruker, CA) with a nominal spring constant of 0.24 Nm⁻¹ and a nominal tip radius of 2 nm were used and imaging was performed in PBS buffer pH 7.4 containing CaCl₂ (0.5 mM) and MnCl₂ (0.5 mM). Images were processed by flattening using NanoScope software to remove the background slope. The roughness analysis of the images was done with the NanoScope software.

Results and discussion

Recognition-driven layer-by-layer assembly of multi-protein interfacial architectures

The platform to build-up the supramolecular assemblies was constructed by modifying gold films with mannose groups following the experimental protocol described by Willner and co-workers for the immobilization of Con A *via* carbohydrate-lectin interactions.¹⁷ Gold-coated glass slides were treated with an ethanolic solution of cystamine. The resulting self-assembled cystamine monolayer-modified surface was then modified with isothiocyanatophenyl α -D-mannopyranoside in phosphate buffer (pH = 7.4), to yield the thiourea monosaccharide monolayer-modified electrodes of phenyl α -D-mannopyranoside.

Once the surfaces were functionalized, we proceeded to monitor the formation of the glycoassemblies on the gold surfaces and estimate the mass coverage of the respective building blocks under saturation conditions, *i.e.*, 1 μM protein.¹⁸ The multi-layer assembly was created using different building blocks including the lectins (redox-active and nonelectroactive) and the glycoproteins (HRP and GOx). We used a quartz crystal microbalance with dissipation monitoring (QCM-D) to follow the growth of the multilayer assembly driven by the molecular recognition between the corresponding building blocks.¹⁹ Fig. 1 shows the layer-by-layer multi-protein assembly of Con A, HRP and GOx as measured by QCM-D at the third overtone. The protein layers were assembled from 1 μM solutions in 0.1 M PBS buffer. A rinsing step between the assemblies of the different layers was included in order to remove any unbound protein remaining on the substrate. A baseline was first measured for the mannosylated gold coated quartz crystal in contact with 0.1 M PBS buffer. Then, the Con A solution was injected into the QCM-D chamber. A rapid decrease in frequency was observed due to the conjugation of the protein onto the ligand-modified substrate. The Con A solution was in contact with the mannose-terminated surface for approximately 15 min, thus enabling the formation of a protein layer on the Au surface. The frequency changes were accompanied with small (increasing) changes in dissipation

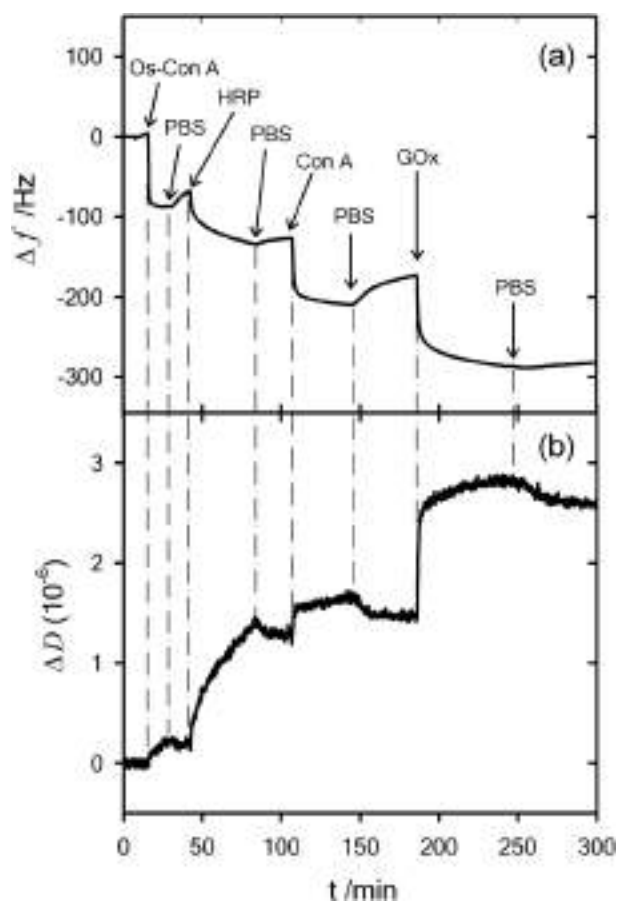


Fig. 1 QCM response on (a) frequency and (b) dissipation at the overtone number $n = 3$ (15 MHz) describing the layer-by-layer growth of the protein assembly.

indicating that the first Con A layer resembles a rather compact and rigid film. After rinsing, the buffer solution was replaced by the HRP solution, which was acting as a “multivalent” glyco-building block bioconjugating the Con A layer.²⁰ In contrast to the first Con A layer, the recognition-driven assembly of HRP displayed a slower decrease in frequency and a significant increase in dissipation. The increase in energy dissipation might be ascribed to the non-rigid layer structure of HRP onto the Con A layer. Rinsing with buffer did not evidence major changes in frequency and only slight changes in dissipation. These slight changes in dissipation could be attributed to relaxation or conformational changes of the HRP layer resulting in a more compact assembly.²¹ Once rinsed, we assembled the second Con A layer onto the HRP layer. The initial exposure to the Con A solution led to a rapid decrease in frequency followed by a slight steady decrease. The assembly of the second layer of Con A only described a slight increase in dissipation, implying that the protein contributes to the dissipative characteristics of the interfacial architecture to a minor extent. After rinsing, the assembly of the GOx layer on the Con A-terminated protein film was accomplished. This led to a significant decrease in frequency accompanied by a sharp increase in dissipation. Further rinsing with buffer demonstrated that the glycoprotein was efficiently anchored to the supramolecular architecture and no weakly bound proteins were at the sensor surface.

The results indicate that by increasing the number of layers the viscoelastic characteristics of the interfacial architecture are increased. The recognition-driven multilayer growth of the protein assembly was also characterized by surface plasmon resonance spectroscopy (SPR).²² Fig. 2 shows the different

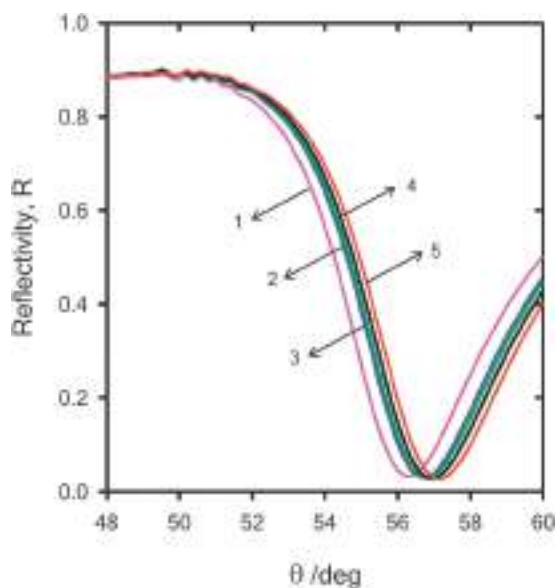


Fig. 2 Reflected intensity as a function of the angle-of-incidence scan (θ) plot describing the recognition-directed assembly of the multilayered protein film on the Au electrode. The reflectivity shifts evidence the sequential assembly of the different molecular building blocks into the interfacial architecture. The different reflectivity curves correspond to: (1) mannosylated gold surface, (2) Au/Os-Con A, (3) Au/Os-Con A/HRP, (4) Au/Os-Con A/HRP/Con A, and (5) Au/Os-Con A/HRP/Con A/GOx.

reflectivity curves obtained during the layer-by-layer growth of Con A, HRP and GOx mediated by the polyvalent carbohydrate–lectin interactions between the constituting building blocks. SPR response originates from refractive index changes as water is replaced by the biomolecules and the shifts in the minimum of the angular θ scans of reflected intensity ($\Delta\theta$) reflect the sequential assembly of the different building blocks into the interfacial architecture. This gives clear evidence that the multivalent character of the glycoproteins and the lectin enables the creation of a biorecognizable interface on top of the Con A layer where the upmost glycoprotein is able to biorecognize the carbohydrate binding site ligands without affecting the stability of the supramolecular architecture or the recognition properties of the protein. In close analogy to polyelectrolyte multilayers, where each polyion is responsible for the charge reversal of the interface, the multivalent character of each building block is responsible for reversing the ligand/receptor character of the interface. It is worth mentioning that these reflectivity shifts can also be correlated to mass coverage values of the respective proteins and, hence, the SPR technique will be used to quantify the protein assembly in each sequential step of the multilayer growth. In a similar way, differences in mass uptake obtained from QCM and SPR experiments were used to offer a rough estimate of the solvent incorporated into the film after assembling each protein layer.²³

Glycoenzyme “wiring” to electrode supports by redox-active lectin layers. Recognition-driven construction of chemoresponsive biointerfaces

So far, we have demonstrated that lectin–carbohydrate interactions can be exploited as a powerful driving force to assemble multiprotein interfacial architectures. Next, we will study the bioelectrochemical features of the protein modified electrodes as well as the routes to manipulate the chemoresponsive activity of the multiprotein assemblies. In our experimental scenario, each building block contributes to a particular function of the whole assembly (Fig. 3). GOx is the biorecognition element that catalyzes the chemical transformation of the chemical stimulus, *i.e.*: glucose, HRP is the transducing bioactive element that reduces the H_2O_2 produced in the primary reaction, Con A acts as a biosupramolecular bridge connecting the glycoprotein layers and Con A-Os as an electron-conducting phase enabling the assembly and electrical wiring of HRP. Bienzyme bioelectrodes combining HRP with GOx were formerly proposed by Kulys *et al.*²⁴ during the early 1980s to detect glucose and since then many bienzyme approaches were developed.²⁵

The use of layer-by-layer electrostatic assembly of redox-labeled polyelectrolytes and redox glycoproteins led to interesting biosensing architectures,²⁶ but these electrostatic assemblies were almost limited to GOx. Even if the construction of bienzymatic assemblies in polyelectrolyte multilayers on flat substrates and colloids has been demonstrated for several enzymes,²⁷ its extension to redox polyelectrolytes in the absence of crosslinking agents has been so far scarce.²⁹ Along these lines, other groups explored the use of covalent binding to assemble monolayers²⁸ and multilayers of HRP and GOx mediated by redox-active metal nanoparticles.²⁹ However, it is well known that in some cases a deliberate covalent modification in an

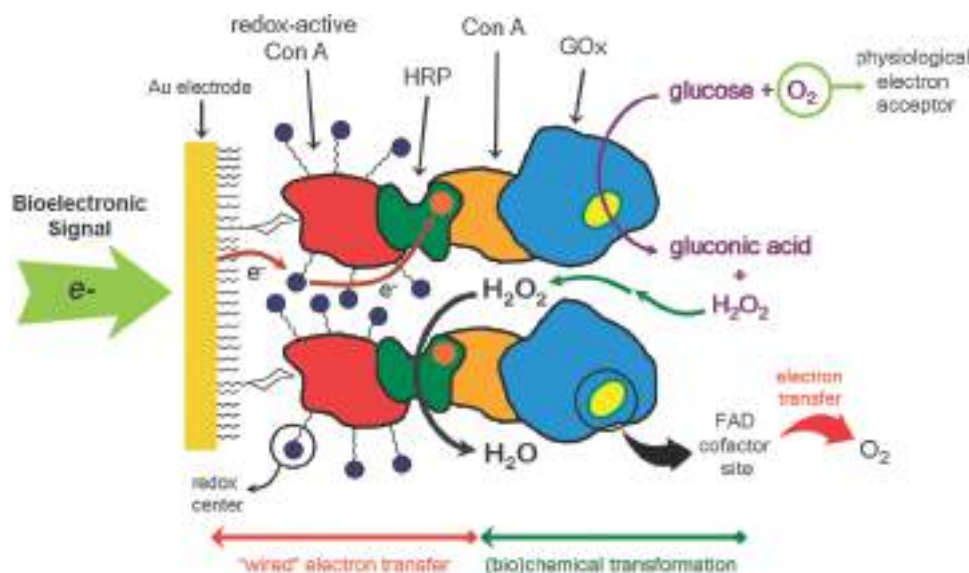


Fig. 3 Illustrative schematic of the glucose-responsive LbL-grown film spontaneously assembled *via* molecular recognition processes. The figure describes the constituting building blocks participating in the generation of the bioelectronic signal in the presence of glucose: redox-active Con A, HRP, Con A and GOx.

uncontrolled way can induce conformational changes in the enzyme, which could be accompanied with a significant loss of enzymatic activity.³⁰ Typically, covalent multipoint attachment is more likely to disrupt the folding and functionality of the native biomolecule if essential groups are involved in the binding process.³¹ With this in mind, the recognition-driven assembly technique represents an interesting and attractive alternative due to its simplicity and versatility. This is applicable to native glycoproteins and is exclusively based on the different supramolecular interactions that living organisms use to form molecular complexes, which in turn lead to fast and easy immobilization protocols avoiding the deterioration of the catalytic activity of the enzymes.

However, important limitations arise when the “biosupramolecular” approach is intended to be implemented at electrochemical interfaces to integrate redox glycoproteins. Electrical communication between the glycoenzyme and the electrode is not feasible because the non-electroactive lectin acts as an insulating biorecognizable spacer, not only inhibiting the shuttling of electrons across the interface but also demanding the use of leachable diffusional redox mediators in solution to overcome this limitation. Recently, we have demonstrated that controlled decoration of Con A with Os(II) redox-active complexes enables the construction of electroactive biosupramolecular building blocks displaying carbohydrate recognition properties similar to those observed in native Con A.¹⁴ To explore this redox-biosupramolecular concept, we have assembled protein multilayers in a sequential order: Os-Con A/HRP/Con A/GOx, on mannosylated gold electrodes. To quantify the amount of lectin and glycoenzyme incorporated into the interfacial bioconjugate, we monitored the sequential immobilization process using SPR as was previously described. These reflectivity shifts were correlated to mass coverage as indicated in Table 1. Con A bearing 12 redox centers retains its ability to bind not only the mannose groups on the electrode surface but the glycosidic portion of the enzyme as well.

Table 1 Surface coverage of proteins constituting the Au/Os-Con A/HRP/Con A/GOx assembly, as determined by SPR. The table also offers rough estimates of the amount of solvent (water) incorporated in the multilayer film after the assembly of each layer. These rough estimates were obtained from differences in mass uptake derived from QCM and SPR experiments

Protein layer	Building block	Protein coverage [pmol cm ⁻²]	Amount of solvent [ng cm ⁻²]	Mass percentage of water in the protein layer
1	Os-Con A	1.92	~174	~44
2	HRP	0.61	~271	~72
3	Con A	0.56	~287	~81
4	GOx	0.90	~360	~71

In this interfacial architecture the innermost lectin layer (Os-Con A) is responsible for acting not only as a “*biosupramolecular glue*” to facilitate the robust and easy attachment of HRP without affecting its catalytic activity but also as an electron-conducting phase to enable the electrical communication between the prosthetic group of the enzyme and the electrode support (Fig. 3). Conversely, the role of the outermost lectin layer (native Con A) is only to assemble the HRP and GOx in close proximity *via* robust, specific noncovalent interactions. We used cyclic voltammetry to study the chemoresponsive bioelectrocatalytic properties of the supramolecular assemblies of HRP/Con A/GOx formed on the redox-tagged Con A-modified Au electrodes. Fig. 4 describes the linear-sweep voltammograms of the Au/Os-Con A/HRP/Con A/GOx interfacial architecture from 0.5 to 0.0 V (*vs.* Ag/AgCl) in the absence and in the presence of increasing amounts of glucose. The voltammetric response eloquently illustrates not only the glucose responsiveness to micromolar concentrations but also the sensitivity of the biosupramolecular enzymatic electrode due to the closeness of both enzymes, minimizing mass transport limitations of the hydrogen peroxide generated by GOx and consumed by HRP, revealing that an efficient biomimetic signal chain operates within the assembly (Fig. 3).

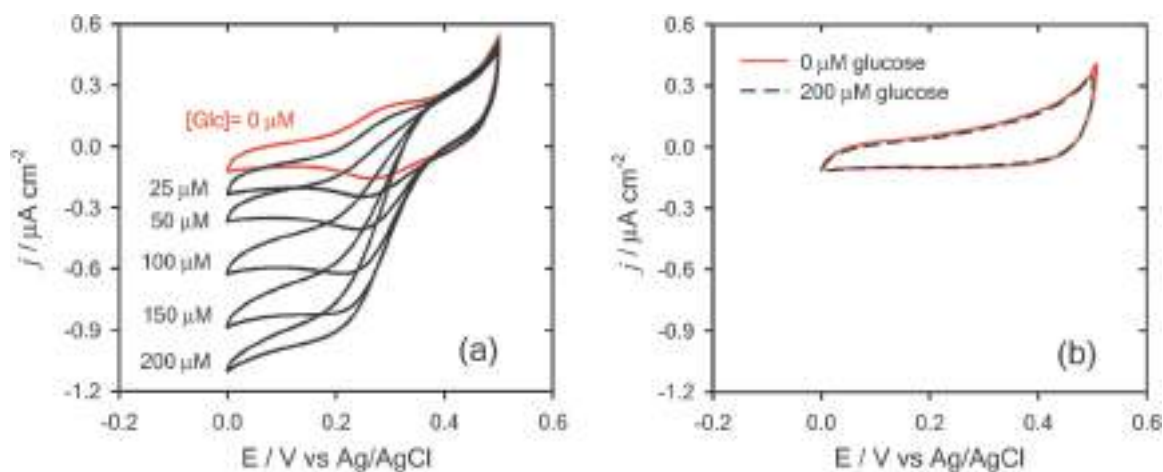


Fig. 4 (a) Cyclic voltammograms describing the electrochemical response of Au/Os-Con A/HRP/Con A/GOx assemblies in the presence of increasing amounts of glucose. (b) Blank experiments describing the electrochemical response of Au/Con A/HRP/Con A/GOx assemblies in the absence (red trace) and in the presence of 200 μM glucose (dashed line). Phosphate buffer, pH 7.4, $T = 295 \text{ K}$, scan rate = 10 mV s^{-1} . The term “Os-Con A” refers to $(\text{Os}(\text{bpy})_2\text{Clpy})^+ \text{-PEG}_{12}\text{-Con A}$.

In other words, a consecutive sequence of biochemical transformations involving electron transfer processes and mass transport takes place in the organized protein assembly. As expected, control experiments performed on analogous supramolecular assemblies that contained native (non-electroactive) Con A revealed no electrocatalytic activity (Fig. 4b). This experimental evidence corroborates that the $\text{Os}^{\text{II/III}}$ -modified Con A layer serves not only as a bioaffinity platform to anchor the peroxidase but also as a conducting phase to electrically connect its heme center to the Au electrode.

Recognition-directed assembly introduces a very simple means to locate each pre-designed building block into the interfacial architecture in an arbitrary manner. As a result, topological, chemical and functional aspects of the protein assembly can be easily explored by exchanging building blocks. For example, replacing the native Con A in the outermost lectin layer by redox-active Con A strongly affects the functional properties of the bienzyme bioelectrode. At first sight, one should expect that upon increasing the electroactivity of the protein assembly the electrochemical response to the chemical stimulus should be enhanced. However, the experimental evidence revealed that this is not the case. Fig. 5 depicts a comparative chart including the cyclic voltammograms corresponding to multiprotein assemblies in different configurations in the presence of 200 μM glucose. It is clear that the presence of Os-Con A in the innermost layer interfacing HRP with the gold electrode leads to a better bioelectrocatalytic activity as compared with the protein assembly presenting Os-Con A on each lectin layer. To interpret these data we need to consider that in the case of Au/Os-Con A/HRP/Os-Con A/GOx assembly both glycoproteins are in close proximity to Os centers. In this scenario GOx can catalyze the glucose oxidation reaction using O_2 or Os^{III} as a mediator. The O_2 is the natural redox partner in the re-oxidation process of the enzyme, exhibiting a rate constant twice the value of the osmium complex ($1.6 \times 10^6 \text{ M}^{-1} \text{ s}^{-1}$ (ref. 32) and $8.2 \times 10^5 \text{ M}^{-1} \text{ s}^{-1}$ (ref. 33) respectively). Consequently, if the transport of O_2 to the enzyme is not limited, then the generation of H_2O_2 will

play a determinant role in the functional features of the bioelectrode and consequently the protein assembly will display a superior sensitivity to the chemical stimulus, *i.e.*: glucose. On the other hand, if Os^{III} centers located in the surroundings of the GOx layer compete with O_2 for mediating the glucose oxidation reaction, then the generation of H_2O_2 will be lower, and consequently the interfacial assembly will display a limited sensitivity to glucose.

In our case, the experimental evidence indicates that Os^{III} centers indeed compete with O_2 as redox mediators of the glucose oxidation. Otherwise, if glucose reaction proceeds with O_2 as the only mediator we should observe superior biocatalytic behaviour in Au/Os-Con A/HRP/Os-Con A/GOx rather than in Au/Os-Con A/HRP/Con A/GOx. Other examples of the order imposed by the construction method can be observed in the amperometric response when Os-Con A is exchanged with native Con A. When only native Con A is used as a building block (magenta voltammogram in Fig. 5) no catalytic response is observed since the enzymes are not able to exchange directly electrons with the electrode surface. Furthermore, the Au/Con A/HRP/Os-Con A/GOx assembly (Fig. 5, green trace) presents an unexpected behaviour. Given the sequence employed for its construction, a similar response to that observed for the Au/Con A/HRP/Con A/GOx assembly (Fig. 5, magenta trace) would be expected since the non-electroactive lectin should act as an insulating barrier. The observed response, although very moderate compared with other architectures, can be explained by considering that after the Con A layer assembly, the successive protein building blocks assemble as submonolayers. Additionally, the high water content within the assembly (see Table 1) suggests an open structure.³⁵ These characteristics denote that layer interpenetration is, at some level, facilitated allowing osmium centers from the Os-Con A layer to access the electrode surface and consequently mediate the reduction of H_2O_2 catalyzed by HRP. Later on in the next section we will discuss how this phenomenon can be minimized by assembling dextran as a promoter for the

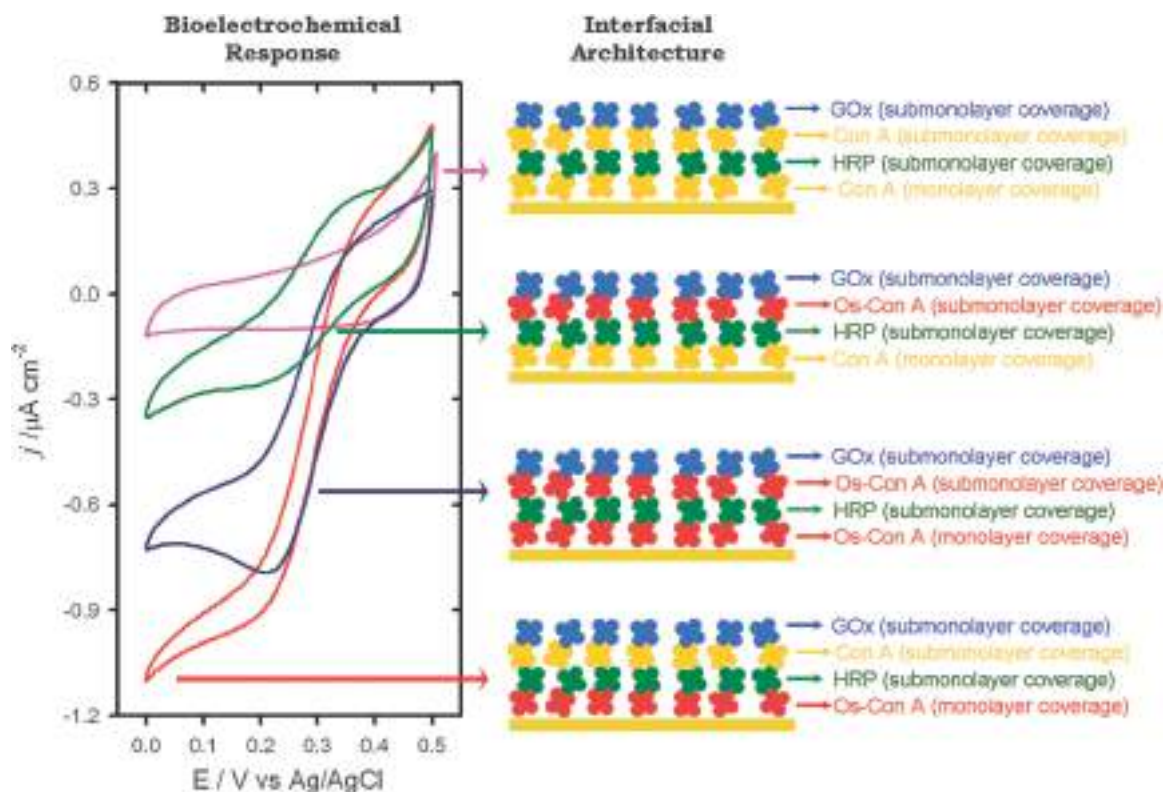


Fig. 5 Comparative chart displaying the voltammetric response of Au/Con A/HRP/Con A/GOx (magenta trace), Au/Con A/HRP/Os-Con A/GOx (green trace), Au/Os-Con A/HRP/Os-Con A/GOx (blue trace) and Au/Os-Con A/HRP/Con A/GOx (red trace) in the presence of 200 μM glucose. Phosphate buffer, pH 7.4, $T = 295 \text{ K}$, scan rate = 10 mV s^{-1} . The figure also includes an idealized picture of the constructed interfacial architectures under different spatial configurations. The assembly sequence of Con A, Os-Con A, HRP and GOx and the building blocks is indicated in different colors. The nature of the coverage in brackets is relative to a closely packed monomolecular layer of protein considering the molecular size of the proteins and the amount of water trapped in the film (see Table 1).³⁴

creation of a physical barrier between biochemical and transduction processes.

In this section we have shown that recognition-driven LbL assembly enables the formation of multicomponent protein films in which electroactive sites and biofunctional entities can be located within the multilayered interfacial nanostructure in an arbitrary manner. This paves the way to the facile creation of biosupramolecular systems exhibiting structural and active components that ultimately will lead to concerted functions when put together in an organized way. However, when dealing with supramolecular systems exhibiting nanoscale dimensions it is crucial to understand the critical interplay between topological and functional aspects. In the previous example we have seen that increasing the electroactivity of the assembly has a deleterious effect on the generation of the biomimetic signal chain. This fact reflects that an actual rational design of biosupramolecular multilayered assemblies is necessary to achieve full potential of the active elements.

A “biomolecular LEGO Kit” to create multi-protein functional bioelectrodes – “brick-by-brick” nanoconstruction of biomimetic signal chains

As we discussed in the previous section our biosupramolecular assemblies exhibit structural and active components. GOx is responsible for performing the primary biochemical transformation

whilst HRP acts as a transducing bioactive element. We have also observed that the electroactivity of the innermost lectin layer plays a fundamental role in the electrochemical transduction of the chemical stimulus and, in contrast, the presence of Os centers in the outermost Con A layer decreases the catalytic efficiency of the biomolecular assembly. Hence, in order to improve the design of the biomimetic signal chain we have created a multilayer assembly in which the innermost layers were constituted of two Os-Con A/HRP bilayers in order to boost the electrochemical readout of the H_2O_2 diffusing into the surroundings of the peroxidase layers.

Fig. 6 shows the cyclic voltammograms corresponding to Au/(Os-Con A/HRP)₂/Con A/GOx. The voltammetric response indicates that the increase in the content of HRP and Os-Con A in the innermost region of the biofilm (Fig. 6a and b) has a marked effect on the efficiency of the biomimetic signal chain, as compared with Au/Os-Con A/HRP/Con A/GOx assemblies (Fig. 4a). Furthermore, time-resolved amperometric measurements (Fig. 6c) clearly reveal that the sensitivity of assemblies containing two Os-Con A/HRP inner bilayers is significantly higher than those assemblies containing only one Os-Con A/HRP inner bilayer. Next, we estimated the sensitivity of the biomolecular assembly by plotting the biocatalytic current as a function of the glucose concentration. These values corresponded to $4.6 \text{ nA cm}^{-2} \mu\text{M}^{-1}$ and $7.6 \text{ nA cm}^{-2} \mu\text{M}^{-1}$ for assemblies containing one and two

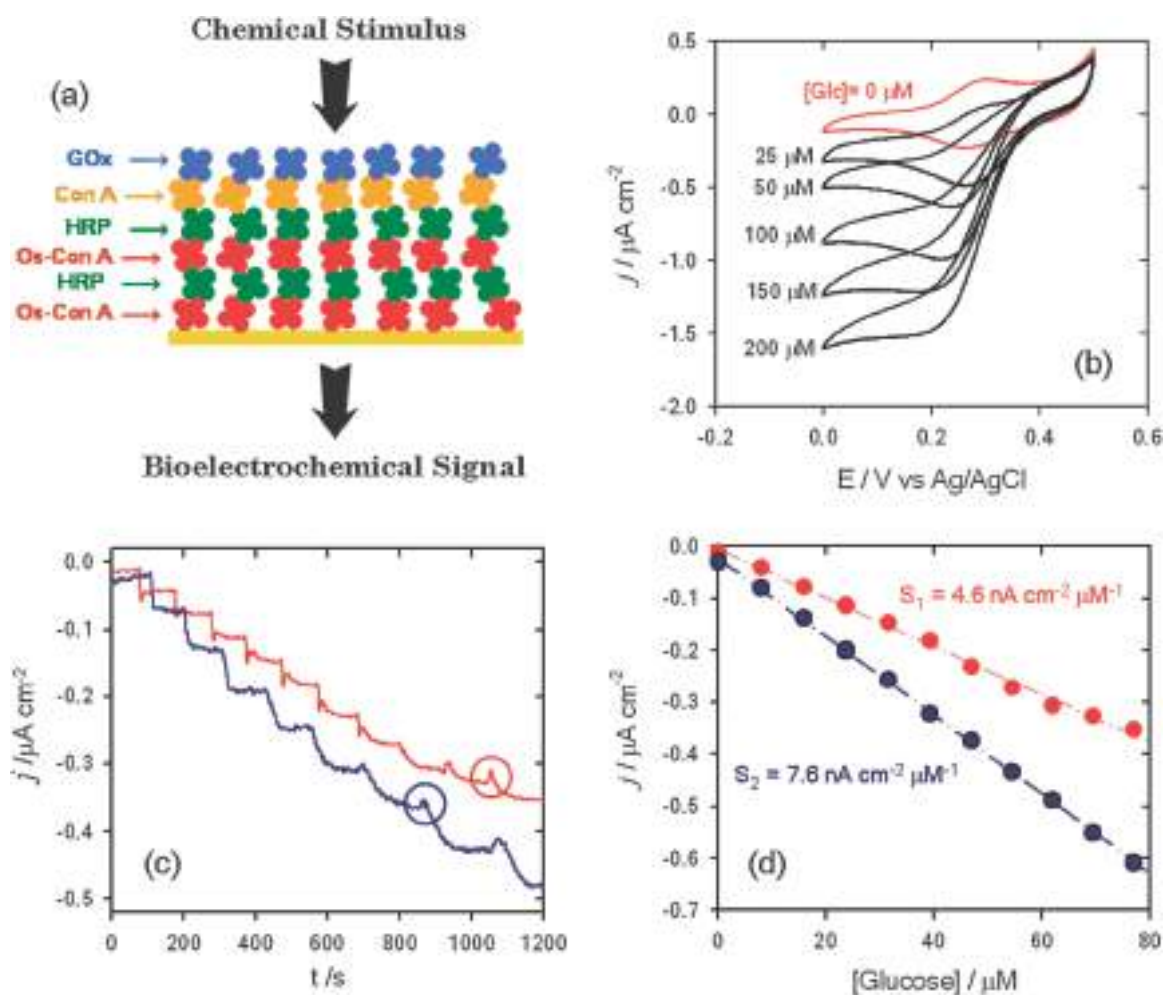


Fig. 6 (a) Simplified schematic describing the spatial localization of native and redox-active Con A within the interfacial architectures. (b) Cyclic voltammograms describing the electrochemical response of Au/(Os-Con A/HRP)₂/Con A/GOx assemblies in the presence of increasing amounts of glucose. Phosphate buffer, pH 7.4, $T = 295$ K, scan rate = 10 mV s^{-1} . (c) Chronoamperometric response at 0 V vs. Ag/AgCl in phosphate buffer, pH 7.4, $T = 295$ K, of Au/Os-Con A/HRP/Con A/GOx (red trace) and Au/(Os-Con A/HRP)₂/Con A/GOx (blue trace) assemblies upon successive addition of a substrate. Each cathodic current increase is correlated to an $\sim 7 \mu\text{M}$ increase in glucose. The circles indicate the presence of an undesired pathway for the electrochemical transduction of glucose oxidation designated as “anodic spikes”. (d) Bioelectrocatalytic currents measured on Au/Os-Con A/HRP/Con A/GOx (red trace) and Au/(Os-Con A/HRP)₂/Con A/GOx (blue trace) assemblies as a function of substrate concentration.

inner Os-Con A/HRP bilayers, respectively (Fig. 6d). Hence, changing from a one-bilayer to a two-bilayer configuration leads to a 65% increase in “sensitivity”. However, it is worthwhile noticing that changing from a one- to a two-bilayer configuration does not necessarily mean that the content of Os-Con A and HRP increases 100%. The actual surface coverage of the proteins incorporated during the sequential assembly was estimated by SPR (Table 2).

Table 2 Surface coverage of proteins constituting the Au/(Os-Con A/HRP)₂/Con A/GOx assembly, as determined by SPR

Protein layer	Building block	Coverage [pmol cm^{-2}]
1	Os-Con A (1st layer)	1.71
2	HRP (1st layer)	0.57
3	Os-Con A (2nd layer)	0.51
4	HRP (2nd layer)	0.24
5	Con A	0.54
6	GOx	0.90

Results depicted in Table 2 suggest that upon increasing the total surface coverage of HRP from 0.57 to $0.81 \text{ pmol cm}^{-2}$ ($\sim 33\%$) the sensitivity of the assembly increased nearly 65%. For the sake of comparison we have normalized both sensitivities (one- and two-bilayer configurations) against total HRP coverage. Normalized results are 7.54 and $9.38 \text{ nA } \mu\text{M}^{-1} \text{ pmol}^{-1}$ (pmol refers to HRP picomole) for one-bilayer and two-bilayer assemblies, respectively, indicating that upon increasing the number of layers the redox efficiency of the protein assembly improves. To address this point in more detail it is important to analyze the intrinsic electroactivity of the supramolecular assembly. The electrochemical charge values associated with the voltammetric response of the supramolecular assemblies in the absence of glucose gives a quantitative estimation of the density of electroactive Os sites “wired” to the gold electrode (Fig. 6b, red trace). In the case of Au/Os-Con A/HRP/Con A/GOx this value is $0.63 \mu\text{C cm}^{-2}$ or 3.9×10^{12} redox sites per cm^2 (6.5 pmol cm^{-2}) “wired” to the underlying gold electrode.

The combination of electrochemical and SPR measurements enables a good estimation of the actual population of “electroactive” Os sites. The average number of redox sites per Con A is 12 (as estimated from MALDI-ToF¹⁴) and the surface coverage of the redox-tagged Con A is 1.92 pmol cm⁻². This value corresponds to 23 pmol cm⁻² (surface coverage of Os centers $\equiv 12 \times 1.92$ pmol cm⁻²). A direct comparison of electrochemical and SPR-derived values indicates that only 28% of the Os centers are actually connected to the underlying electrode surface. However, when the same comparison was done with the Au/(Os-Con A/HRP)₂/Con A/GOx assembly we estimated that $\sim 70\%$ of the redox centers are connected to the gold electrode. These experimental results suggest the presence of “percolation effects” within the protein film that might lead to better redox connectivity upon increasing the number of Os-Con A/HRP bilayers in the inner region of the biomolecular assembly. Or, in other words, the improved electrical connectivity between the redox mediators leads to an enhanced electrochemical transduction of the chemical stimulus.

However, a careful look at the amperometric response of the bioelectrode reveals intriguing features related to the glucose responsiveness of the heteroprotein interfacial architecture. Upon increasing the concentration of glucose in the electrolyte solution “anodic spikes” followed by a slow current stabilization started to appear in the chronoamperometric recordings (Fig. 6c). This effect is more significant immediately after adding

glucose to the electrolyte solution, which indicates that the local concentration of substrate can play an important role. For instance, this tendency became even more pronounced at higher glucose concentrations. This observation can be attributed to the presence of GOx in close proximity to a number of Os centers. After the monolayer of Os-Con A, the subsequent protein building blocks are assembled under submonolayer conditions allowing the direct contact of GOx with Os centers present in the Os-Con A layers. GOx in the reduced form can react with Os^{III} generated through the reaction of the HRP, thus promoting a temporary decrease in magnitude or extent of the cathodic electrochemical signal arising from the biomimetic signal chain. Hence, the presence of Os centers in the surroundings of the GOx layers introduces an undesired pathway for the electrochemical transduction of the biochemical transformations (Fig. 7a). A similar scenario has been already described in biozymatic electrodes by other authors.³⁶ Therefore, an optimal conversion of the biomimetic signal chain into an electronic signal would imply “decoupling” of the biochemical process occurring in the outer region of the assembly (glucose oxidation in the presence of GOx and physiological O₂) from the “wired” interfacial electron transfer in the presence of HRP in the innermost layers of the interfacial bioconjugate.

To this end, we explored the use of dextran as a permeable interlayer enabling the physical separation of the Os centers attached to the innermost electroactive Con A from the GOx

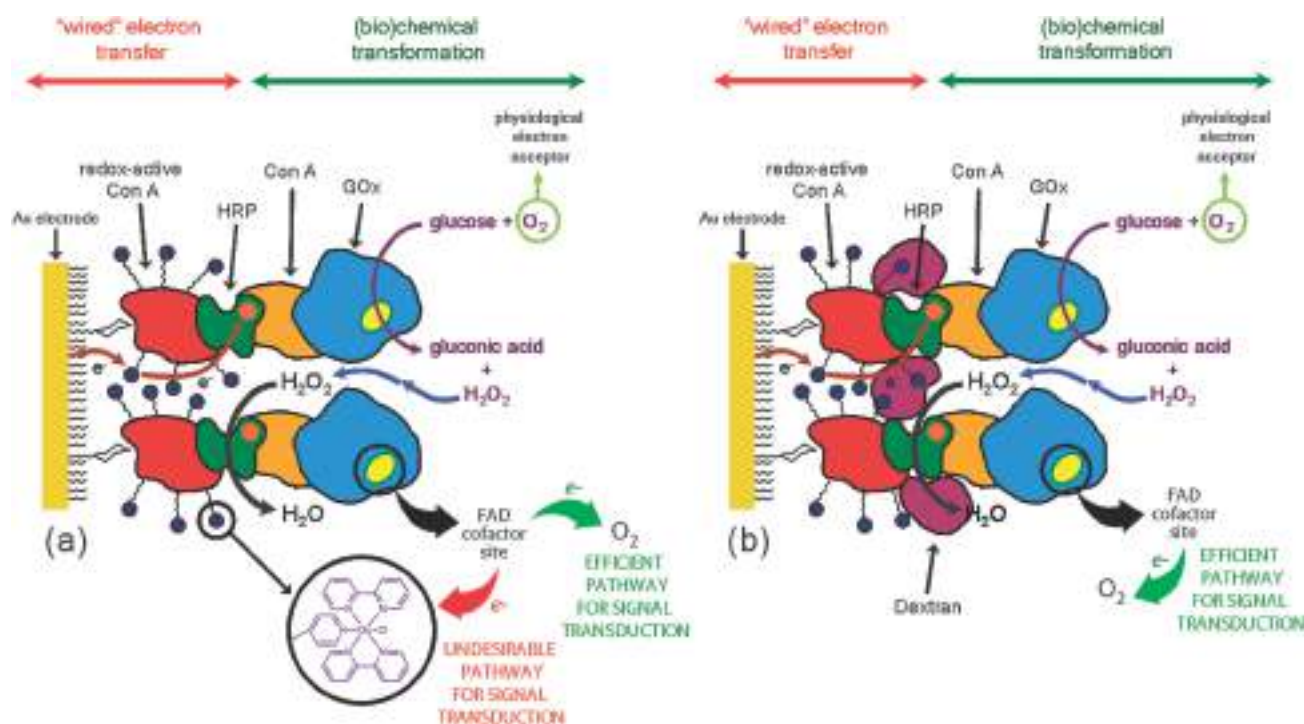


Fig. 7 Schematic depiction of the different scenarios in which the biomimetic signal chain takes place. (a) The presence of GOx in the reduced form can react with neighboring Os^{III} sites generated through the reaction of the HRP. This interfacial configuration can promote a temporary decrease in the magnitude of the cathodic signal arising from the biomimetic signal chain due to undesirable pathways for signal transduction. (b) An optimal quantitative conversion of the biomimetic signal chain into an electronic signal implies glucose oxidation in the presence of GOx and physiological O₂ without any interference from the neighboring Os^{III} species. This can be achieved using bio-assembled dextran layers as physical barriers separating the Os redox centers from the FAD cofactor sites in the GOx layer without hindering the free diffusion of H₂O₂ into the “wired” HRP layers.

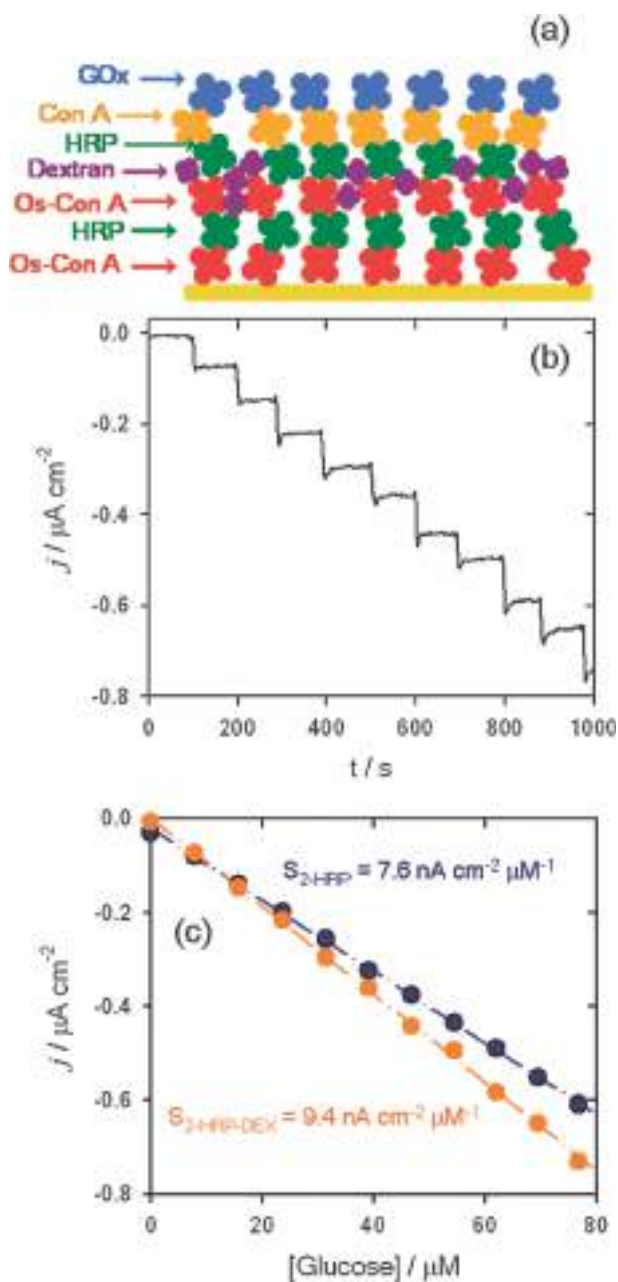


Fig. 8 (a) Simplified schematic describing the spatial localization of native and redox-active Con A and dextran within the interfacial architecture. (b) Chronoamperometric response at 0 V vs. Ag/AgCl in phosphate buffer, pH 7.4, $T = 295$ K, of Au/(Os-Con A/HRP)₂/dextran/Con A/GOx assembly upon successive addition of a substrate. Each cathodic current increase is correlated with an $\sim 7 \mu\text{M}$ increase in glucose. (c) Bioelectrocatalytic currents measured on Au/(Os-Con A/HRP)₂/dextran/Con A/GOx (orange symbols) and Au/(Os-Con A/HRP)₂/Con A/GOx (blue symbols) assemblies as a function of substrate concentration.

layer assembled on top of the protein film (Fig. 8a). Dextran is a polysaccharide that specifically binds to Con A.³⁷ For instance, it has been reported that biospecific binding between Con A and dextran leads to the formation of a hydrogel-like system which changes its viscosity in response to free glucose concentration.³⁸ Fig. 8b describes the chronoamperometric

response of a multiprotein assembly incorporating dextran (molecular mass: 40 kDa – surface coverage: $0.31 \text{ pmol cm}^{-2}$, as determined by SPR) as a permeable interlayer, *i.e.*: Au/(Os-Con A/HRP)₂/dex/Con A/GOx, in the presence of increasing amounts of glucose. It is evident that the presence of dextran enables better defined and more stable glucose response as revealed by the biocatalytic amperometric recording (Fig. 8b) as well as better sensitivity – see Fig. 8c, biocatalytic current as a function of the glucose concentration. Even though dextran does not play an active role in the assembly, its role as a structural component is decisive to optimize the electronic readout and sensitivity of the biomimetic signal chain. This would imply, at first sight, that recognition-directed assembly of dextran on exposed sites of the Os-Con A layer would fill the voids of the HRP/Os-Con A architecture and, consequently, may help to separate the Os redox centers from the FAD cofactor sites in the GOx layer without hindering the free diffusion of H₂O₂ into the innermost “wired” layers of the biomolecular assembly (Fig. 7b).

To further explore this hypothesis based on the use of dextran as a structural building block we carried out *in situ* atomic force imaging during the sequential layer-by-layer assembly of the protein multilayers. Fig. 9 shows *in situ* AFM images of a gold electrode consecutively modified with Os-Con A, HRP, dextran, Con A and GOx.

It is clear that consecutive protein assembly promotes changes in the topography of the surface-confined bioconjugate. Structural characteristics of the supramolecular assembly at different growth stages are clearly evidenced by the *in situ* imaging technique. Topographic imaging of the biosupramolecular LbL assembly reveals roughness changes upon multilayer growth. Sequential addition of Os-Con A and HRP is reflected as a decrease in the roughness (RMS) of the film (Table 3).

The preservation of the Au roughness when the mannose derivative is adsorbed indicates that its adsorption follows, practically in an atomic level, the topography of the gold surface. On the other hand, the assembly of the Con A and HRP layers levels off the surface topography. This could be ascribed to the filling of the voids as the number of protein layers is increased. It is interesting to note the differences observed when a second layer of Con A is added compared with dextran (see Table 3). The first one, a globular 104 kDa protein promotes an increase in surface roughness; while the addition of dextran, a branched polymer, does not produce appreciable changes in the roughness. This behavior can be understood by considering dextran as a flexible polymer architecture that can fill the voids left by the peroxidase. Recent work of Venturoli and Rippe³⁹ based on a comparative analysis between dextran and globular proteins revealed that whereas globular proteins seem to behave in a way similar to hydrated hard spheres, dextran behaves like a flexible random coil. *In situ* AFM imaging supports our hypothesis that the dextran interlayer optimizes structural features of the complex biosupramolecular assembly. Recognition-directed assembly of dextran on exposed recognition sites of the Os-Con A/HRP inner bilayer would not only lead to a more homogeneous and compact Con A outer layer but also facilitate the filling of the voids in the Os-Con A/HRP bilayer itself. As a result,

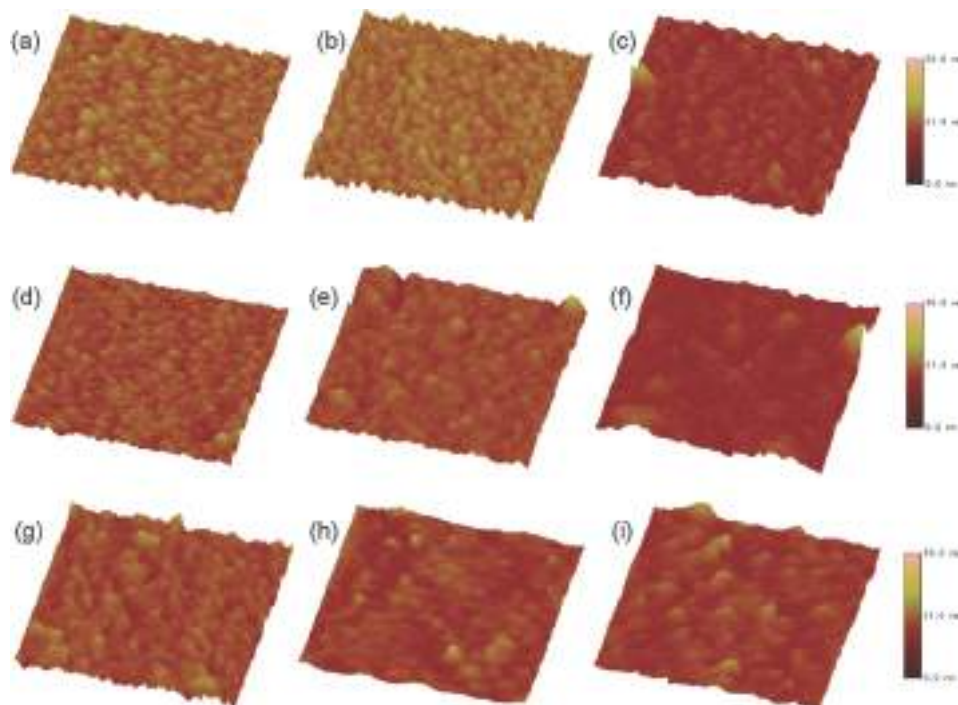


Fig. 9 *In situ* AFM topographic imaging ($1 \times 1 \mu\text{m}^2$, pitch: 45°) describing the biorecognition-driven layer-by-layer assembly of the multiprotein thin film onto the gold electrode. Images correspond to: (a) freshly evaporated Au surface, (b) mannoseylated Au electrode, (c) Au/Os-Con A, (d) Au/Os-Con A/HRP, (e) Au/Os-Con A/HRP/Con A, (f) Au/Os-Con A/HRP/Con A/GOx, (g) Au/Os-Con A/HRP/dextran, (h) Au/Os-Con A/HRP/dextran/Con A, (i) Au/Os-Con A/HRP/dextran/Con A/GOx.

Table 3 Root mean square (RMS) roughness values measured by AFM of protein layers assembled onto the freshly evaporated gold electrode

Layer	Roughness [nm]
Freshly evaporated Au surface	2.8 ± 0.1
Mannoseylated Au electrode	2.9 ± 0.1
Au/Os-Con A	2.5 ± 0.1
Au/Os-Con A/HRP	2.0 ± 0.1
Au/Os-Con A/HRP/Con A	2.5 ± 0.3
Au/Os-Con A/HRP/Con A/GOx	3.9 ± 1.4
Au/Os-Con A/HRP/dextran	2.0 ± 0.7
Au/Os-Con A/HRP/dextran/Con A	2.2 ± 1.0
Au/Os-Con A/HRP/dextran/Con A/GOx.	3.4 ± 1.0

the presence of the dextran interlayer physically hinders the electronic communication between the Os redox centers and the FAD cofactor sites in the GOx protein, but this permeable physical barrier does not preclude the free diffusion of H_2O_2 into the innermost “wired” Os-Con A/HRP layers.

Conclusions

We have successfully fabricated layer-by-layer multiprotein chemoresponsive assemblies by means of multivalent supramolecular carbohydrate–lectin interactions between glycoenzymes and a redox-active Con A. The catalytic response of the assembly toward glucose revealed an efficient electrical communication between the different building blocks along the assembly and the conductive support. Furthermore, a detailed study by cyclic voltammetry and chronoamperometry illustrates that a rational and predefined disposition of the bio-interface elements can be conducted to reach optimum efficiency.

This concept was exhibited by the specific location of the electroactive and non-electroactive Con A inside the assembly. The compartmentalization of the electroactive Con A was an underlying requisite to favor the reaction mediated by O_2 , thus enhancing the glucose-sensitivity of the biointerface.

In another set of experiments we demonstrated that the design of the biomimetic signal chain could be improved by creating a multilayer assembly with two Os-Con A/HRP bilayers as the innermost layer. This was due not only to an increase of Os centers and HRP coverage, but also to the presence of percolation effects within the assembly. This led to an improvement in the population of Os sites electrically connected to the electrode from 28% for the interface with Os-Con A/HRP to 70% for the corresponding one with $(\text{Os-Con A/HRP})_2$, which increased the sensitivity of the assembly by 65%.

An interesting feature displayed by these heteroprotein interfacial architectures was the presence of a non-desirable electrochemical pathway for the electrochemical transduction of glucose oxidation. This process was attributed to the presence of Os centers in the surrounding of GOx. To reduce this phenomenon, we incorporated dextran after the Os-Con A/HRP immobilization step, thus promoting a physical barrier between the electroactive Con A and GOx layers. The resulting supramolecular architecture displayed a better-defined and more stable signal and an enhanced sensitivity toward glucose. Furthermore, *in situ* atomic force microscopy revealed smoother films for the case where dextran was assembled on HRP-terminated films compared to the analogues without dextran. This observation is consistent with the role assigned to dextran as that responsible to fill the voids in the Os-Con A/HRP architecture,

leading to a more homogeneous and compact Con A outer layer, which decouple the biochemical and transduction processes within the assembly.

These results using supramolecular assemblies based on redox-active lectins, polysaccharides and glycoproteins demonstrate the potential of using LbL recognition-directed assembly as a key enabling tool granting access to the rational molecular design of complex multiprotein assemblies. This LEGO-type approach enables us to locally address redox centers and prosthetic groups within the supramolecular bioassembly with nanoscale precision, representing a crucial feature for the nanoconstruction of bioelectronic interfaces as well as the generation of efficient biomimetic signal chains. The elegance of the approach lies in the rational choice of the positioning of individual components that, in turn, determine the overall features of the whole bio-assembly – *different intercalation and 3D organization of the same building blocks lead to major changes in sensitivity*. We envision that this strategy would facilitate the creation of functional soft bio-interfaces displaying specific building blocks at controlled sites in 3D interfacial nanoarchitectures.

Acknowledgements

The authors acknowledge financial support from Max-Planck-Gesellschaft (Max Planck Partner Group for Functional Supramolecular Bioconjugates, INIFTA/MPIP), ANPCyT (PICT Bicentenario 2010-2554, PICT Bicentenario 2010-0457 and PAE 2006 37063, PRH 2007 No. 74, PIDRI No. 74, PICT-PRH 163/08), Centro Interdisciplinario de Nanociencia y Nanotecnología (CINN-ANPCyT-Argentina), Alexander von Humboldt Stiftung (Germany). D.P. and C.v.B. acknowledge CONICET for a postdoctoral and doctoral fellowship, respectively. L.I.P., F.B. and O.A. are CONICET fellows.

References

- (a) G. Decher, *Multilayer Thin Films*, ed. G. Decher and J. B. Schlenoff, Wiley-VCH, Weinheim, 2002, ch. 1, pp. 1–46; (b) X. Shia, M. Shen and H. Möhwald, *Prog. Polym. Sci.*, 2004, **29**, 987; (c) K. Ariga, Q. Ji, J. P. Hill and A. Vinu, *Soft Matter*, 2009, **5**, 3562.
- (a) K. Ariga, J. P. Hill and Q. Ji, *Phys. Chem. Chem. Phys.*, 2007, **9**, 2319; (b) P. Bertrand, A. M. Jonas, A. Laschewsky and R. Legras, *Macromol. Rapid Commun.*, 2000, **21**, 319.
- (a) G. Decher and J. D. Hong, *Ber. Bunsen-Ges.*, 1991, **95**, 1430; (b) G. Decher and J. D. Hong, *Makromol. Chem., Macromol. Symp.*, 1991, **46**, 321.
- (a) G. Cao, H. G. Hong and T. E. Mallouk, *Acc. Chem. Res.*, 1992, **25**, 420; (b) W. B. Stockton and M. F. Rubner, *Macromolecules*, 1997, **30**, 2717; (c) L. Wang, Z. Q. Wang, X. Zhang, J. C. Shen, L. F. Chi and H. Fuchs, *Macromol. Rapid Commun.*, 1997, **18**, 509; (d) Y. L. Liu, M. L. Bruening, D. E. Bergbreiter and R. M. Crooks, *Angew. Chem., Int. Ed. Engl.*, 1997, **36**, 2114; (e) T. Cassier, K. Lowack and G. Decher, *Supramol. Sci.*, 1998, **5**, 309; (f) Y. Lvov, K. Ariga, I. Ichinose and T. Kunitake, *J. Am. Chem. Soc.*, 1995, **117**, 6117; (g) F. Caruso, N. D. Furlong, K. Ariga, I. Ichinose and T. Kunitake, *Langmuir*, 1998, **14**, 4559; (h) T. Shirman, R. Kaminker, D. Freeman and M. E. van der Boom, *ACS Nano*, 2011, **5**, 6553; (i) M. Li, S. Ishihara, M. Akada, M. Liao, L. Sang, J. P. Hil, V. Krishnan, Y. Ma and K. Ariga, *J. Am. Chem. Soc.*, 2011, **133**, 7348; (j) B. Lee, Y. Kim, S. Lee, Y. S. Kim, D. Wang and J. Cho, *Angew. Chem., Int. Ed.*, 2010, **49**, 359; (k) C. Bourdillon, C. Demaille, J. Moiroux and J.-M. Saveant, *J. Am. Chem. Soc.*, 1994, **116**, 10328.
- (a) J.-i. Anzai, Y. Kobayashi, N. Nakamura, M. Nishimura and T. Hoshi, *Langmuir*, 1999, **15**, 221; (b) H. Inoue and J.-i. Anzai, *Langmuir*, 2005, **21**, 8354; (c) K. Sato, Y. Naka and J.-i. Anzai, *J. Colloid Interface Sci.*, 2007, **315**, 396; (d) H. Inoue, K. Sato and J.-i. Anzai, *Biomacromolecules*, 2005, **6**, 27.
- (a) M. J. W. Ludden, X. Li, J. Greve, A. van Amerongen, M. Escalante, V. Subramaniam, D. N. Reinhoudt and J. Huskens, *J. Am. Chem. Soc.*, 2008, **130**, 6964; (b) X. Y. Ling, I. Y. Phang, D. N. Reinhoudt, G. J. Vancso and J. Huskens, *Int. J. Mol. Sci.*, 2008, **4**, 486; (c) M. J. W. Ludden, A. Mulder, R. Tampé, D. N. Reinhoudt and J. Huskens, *Angew. Chem., Int. Ed.*, 2007, **46**, 4104.
- (a) A. L. Martin, B. Li and E. R. Gillies, *J. Am. Chem. Soc.*, 2009, **131**, 734; (b) F. Schröper, A. Baumann, A. Offenhäuser and D. Mayer, *Chem. Commun.*, 2010, **46**, 5295.
- (a) F. Lisdat, R. Dronov, H. Möhwald, F. W. Scheller and D. G. Kurth, *Chem. Commun.*, 2009, 274; (b) R. Dronov, D. G. Kurth, H. Möhwald, F. W. Scheller and F. Lisdat, *Angew. Chem., Int. Ed.*, 2008, **47**, 3000; (c) R. Dronov, D. G. Kurth, H. Möhwald, R. Spricigo, S. Leimkühler, U. Wollenberger, K. V. Rajagopalan, F. W. Scheller and F. Lisdat, *J. Am. Chem. Soc.*, 2008, **130**, 1122.
- (a) I. Willner and E. Katz, in *Bioelectronics: From Theory to Applications*, ed. I. Willner and E. Katz, Wiley-VCH, Weinheim, 2005, ch. 1, pp. 1–13; (b) P. N. Bartlett and C. S. Toh, in *Biosensors: A Practical Approach*, ed. J. Cooper and T. Cass, Oxford University Press, Oxford, 2004, ch. 4, pp. 59–96; (c) A. Badia, R. Carlini, A. Fernández, F. Battaglini, S. R. Mikkelsen and A. M. English, *J. Am. Chem. Soc.*, 1993, **115**, 7053; (d) F. Battaglini, P. N. Bartlett and J. H. Wang, *Anal. Chem.*, 2000, **72**, 502.
- (a) S. David, *The Chemical and Supramolecular Chemistry of Carbohydrates: A Chemical Introduction to the Glycosciences*, Oxford University Press, Oxford, 1997, ch. 15, pp. 250–264; (b) J. W. Becker, G. N. Reeke Jr., G. N. Cunningham and G. M. Edelman, *Nature*, 1976, **259**, 406; (c) R. S. Singh, A. K. Tiwary and J. F. Kennedy, *Crit. Rev. Biotechnol.*, 1999, **19**, 145; (d) H. Lis and N. Sharon, *Chem. Rev.*, 1998, **98**, 637; (e) N. Sharon and H. Lis, *Glycobiology*, 2004, **14**, 53R.
- D. Pallarola, N. Queralto, W. Knoll, O. Azzaroni and F. Battaglini, *Chem.–Eur. J.*, 2010, **16**, 13970.
- (a) Y. Lvov, K. Ariga, I. Ichinose and T. Kunitake, *J. Chem. Soc., Chem. Commun.*, 1995, 2313; (b) Y. Kobayashi and J.-i. Anzai, *J. Electroanal. Chem.*, 2001, **507**, 250; (c) J.-i. Anzai and Y. Kobayashi, *Langmuir*, 2000, **16**, 2851.
- (a) H. Yao and N. Hu, *J. Phys. Chem. B*, 2010, **114**, 9926; (b) H. Yao and N. Hu, *J. Phys. Chem. B*, 2009, **113**, 16021; (c) H. Yao and N. Hu, *J. Phys. Chem. B*, 2010, **114**, 3380; (d) H. Yao and N. Hu, *J. Phys. Chem. B*, 2011, **115**, 6691.
- D. Pallarola, N. Queralto, W. Knoll, M. Ceolín, O. Azzaroni and F. Battaglini, *Langmuir*, 2010, **26**, 13684.
- W. Knoll, *Annu. Rev. Phys. Chem.*, 1998, **49**, 569.
- (a) E. Stenberg, B. Persson, H. Roos and C. Urbaniczky, *J. Colloid Interface Sci.*, 1991, **143**, 513–526; (b) F. Yu, *PhD thesis*, Johannes Gutenberg–Universität Mainz, Germany, http://www.mpip-mainz.mpg.de/knoll/publications/thesis/yl_2004.pdf.
- I. Willner, S. Rubin and Y. Cohen, *J. Am. Chem. Soc.*, 1993, **115**, 4937.
- E. A. Smith, W. D. Thomas, L. L. Kiessling and R. M. Corn, *J. Am. Chem. Soc.*, 2003, **125**, 6140.
- O. Azzaroni, M. Mir and W. Knoll, *J. Phys. Chem. B*, 2007, **111**, 13499.
- (a) M. Farooqi, P. Sosnizza, M. Saleemuddin, R. Ulber and T. Scheper, *Appl. Microbiol. Biotechnol.*, 1999, **52**, 373; (b) M. Farooqi, M. Saleemuddin, R. Ulber, P. Sosnizza and T. Scheper, *J. Biotechnol.*, 1997, **55**, 171; (c) S. Husain, F. Jafri and M. Saleemuddin, *Biochem. Mol. Biol. Int.*, 1996, **40**, 1.
- (a) F. Höök, M. Rodahl, P. Brzezinski and B. Kasemo, *J. Colloid Interface Sci.*, 1998, **208**, 63; (b) C. Larsson, M. Rodahl and F. Höök, *Anal. Chem.*, 2003, **75**, 5080.
- A. Baba, P. Taraneekar, R. R. Ponnappati, W. Knoll and R. C. Advincula, *ACS Appl. Mater. Interfaces*, 2010, **2**, 2347.
- QCM-D response is extremely sensitive not only to the viscoelastic properties but also to the density and thickness of any mass coupled to the quartz crystal surface. In our case, the film is

- constituted of proteins conjugated to the carbohydrate ligand-exposing sensor surface in an aqueous solution. As a consequence, a fraction of solvent is trapped between the adsorbed protein layers. More importantly, this retained water is not strictly “fixed” to the film if we consider that it does not behave as the liquid layer above the film. The QCM detects the solvent that is hydrodynamically coupled to the assembled protein film. In contrast, the SPR response, that originated from refractive index changes as water is replaced by the respective proteins, is mostly proportional to the masses of the adsorbed biomolecules. Recommended reading on this topic: (a) O. Azzaroni, M. Mir and W. Knoll, *J. Phys. Chem. B*, 2007, **111**, 13499–13503; (b) E. Reimhult, C. Larsson, B. Kasemo and F. Höök, *Anal. Chem.*, 2004, **76**, 7211–7220.
- 24 J. J. Kulys, M. V. Pesliakiene and A. S. Samalius, *Bioelectrochem. Bioenerg.*, 1981, **8**, 81.
 - 25 (a) T. J. Obara, M. S. Vreeke, V. F. Battaglini and A. Heller, *Electroanalysis*, 1993, **5**, 825; (b) M. Delvaux, A. Walcarius and S. Demoustier-Champagne, *Biosens. Bioelectron.*, 2005, **20**, 1587; (c) G. Suarez, R. J. Jackson, J. A. Spoors and C. J. McNeil, *Anal. Chem.*, 2007, **79**, 1961.
 - 26 (a) M. Dequaire and A. Heller, *Anal. Chem.*, 2002, **74**, 4370–4377; (b) F. Mao, N. Mano and A. Heller, *J. Am. Chem. Soc.*, 2003, **125**, 4951–4957; (c) P. Scodeller, V. Flexer, R. Szamocki, E. J. Calvo, N. Tognalli, H. Troiani and A. Fainstein, *J. Am. Chem. Soc.*, 2008, **130**, 12690–12697; (d) V. Coman, T. Gustavsson, A. Finkelsteinas, C. von Wachenfeldt, C. Hägerhäll and L. Gorton, *J. Am. Chem. Soc.*, 2009, **131**, 16171–16176.
 - 27 (a) M. Onda, Y. Lvov, K. Ariga and T. Kunitake, *Biotechnol. Bioeng.*, 1996, **51**, 163; (b) M. Onda, Y. Lvov, K. Ariga and T. Kunitake, *J. Ferment. Bioeng.*, 1996, **82**, 502; (c) F. Caruso and C. Schuöler, *Langmuir*, 2000, **16**, 9595–9603; (d) P. Pescador, I. Katakis, J. L. Toca-Herrera and E. Donath, *Langmuir*, 2008, **24**, 14108; (e) S. Disawal, J. Qiu, B. B. Elmore and Y. M. Lvov, *Colloids Surf., B*, 2003, **32**, 145; (f) E. J. Calvo, F. Battaglini, C. Danilowicz, A. Wolosiuk and M. Otero, *Faraday Discuss.*, 2000, **116**, 47.
 - 28 J. M. Abad, M. Vélez, C. Santamaría, J. M. Guisán, P. R. Matheus, L. Vázquez, I. Gazaryan, L. Gorton, T. Gibson and V. M. Fernández, *J. Am. Chem. Soc.*, 2002, **124**, 12845.
 - 29 Y. Sun, Y. Bai, W. Yang and C. Sun, *Electrochim. Acta*, 2007, **52**, 7352.
 - 30 A. G. Mayes, in *Biomolecular Sensors*, ed. E. Gizeli and C. R. Lowe, Taylor & Francis, London, 2002, ch. 4, p. 49.
 - 31 B. Prieto-Simón, M. Campás and J.-L. Marty, *Protein Pept. Lett.*, 2008, **15**, 757.
 - 32 H. J. Bright and M. Appleby, *J. Biol. Chem.*, 1969, **244**, 3625.
 - 33 D. Pallarola, N. Queralto, F. Battaglini and O. Azzaroni, *Phys. Chem. Chem. Phys.*, 2010, **12**, 8071.
 - 34 The molecular dimensions of Con A are reported to be $4.0 \times 7.8 \times 8.0 \text{ nm}^3$ (J. W. Becker, G. N. Reeke Jr., B. A. Cunningham and G. M. Edelman, *Nature*, 1976, **259**, 406). Based on these dimensions a closely packed monomolecular layer of protein corresponds to $(3.8 \pm 1.2) \text{ pmol cm}^{-2}$. Consequently, the surface coverage for the first and second layers of Con A obtained by SPR corresponds to 40–70% and 12–21% of a closely packed monolayer, respectively. Similar calculations for HRP and GOx correspond to 8–12% and 20–30% of a closely packed monolayer of the respective enzyme. The molecular dimensions of HRP and GOx are reported to be $4.0 \times 5.5 \times 5.5 \text{ nm}^3$ (A. Henriksen, A. T. Smith and M. Gajhede, *J. Biol. Chem.*, 1999, **274**, 35005) and $6.0 \times 5.2 \times 7.7 \text{ nm}^3$ (H. J. Hecht, H. M. Kalisz, J. Hendle and R. D. Schmid, *J. Mol. Biol.*, 1993, **229**, 153), respectively. However, all these results do not consider the amount of water within the film, which produces a profound departure from the idealized closely packed monolayer. Consequently, these values have to be taken as an underestimation of the actual situation.
 - 35 (a) M. Rodahl, P. Dahlgqvist, F. Höök and B. Kasemo, in *Biomolecular Sensors*, ed. E. Gizeli and C. R. Lowe, Taylor & Francis, London, 2002, ch. 12, pp. 304–316; (b) C. Larsson, M. Rodahl and F. Höök, *Anal. Chem.*, 2003, **75**, 5080–5087.
 - 36 (a) E. Corton and F. Battaglini, *J. Electroanal. Chem.*, 2001, **511**, 8; (b) R. Mairan and A. Heller, *Anal. Chem.*, 1992, **64**, 2889; (c) T. J. Ohara, M. S. Vreeke, F. Battaglini and A. Heller, *Electroanalysis*, 1993, **5**, 825.
 - 37 (a) I. J. Goldstein, C. E. Hollerman and J. M. Merrick, *Biochim. Biophys. Acta*, 1965, **97**, 68; (b) R. Ballerstadt and J. S. Schultz, *Sens. Actuators, B*, 1998, **46**, 50; (c) R. Yin, J. Han, J. Zhang and J. Nie, *Colloids Surf., B*, 2010, **76**, 483.
 - 38 R. Zhang, M. Tang, A. Bowyer, R. Eissenthal and J. Hubble, *React. Funct. Polym.*, 2006, **66**, 757.
 - 39 D. Venturoli and B. Rippe, *Am. J. Physiol.*, 2005, **288**, F605.